Simulating the Generalized Gibbs Ensemble (GGE): a Hilbert space Monte Carlo approach

Vincenzo Alba[1]

[1] *International School for Advanced Studies (SISSA), Via Bonomea 265, 34136, Trieste, Italy, INFN, Sezione di Trieste*

(Dated: July 12, 2015)

By combining *classical* Monte Carlo and Bethe ansatz techniques we devise a numerical method to construct the Truncated Generalized Gibbs Ensemble (TGGE) for the spin-$\frac{1}{2}$ isotropic Heisenberg (XXX) chain. The key idea is to sample the Hilbert space of the model with the appropriate GGE probability measure. The method can be trivially extended to other integrable systems, such as the Lieb-Liniger model. We benchmark our approach focusing on GGE expectation values of several local observables. The numerical results are in spectacular agreement with the Generalized Thermodynamic Bethe Ansatz (GTBA). Although the method is devised for finite-size chains, finite-size effects decay exponentially with system size, and moderately large chains are sufficient to extract thermodynamic quantities. Remarkably, it is possible to extract in a simple way the steady-state Bethe-Gaudin-Takahashi (BGT) roots distributions, which encode complete information about the GGE expectation values in the thermodynamic limit. Finally, it is straightforward to simulate extensions of the GGE, in which, besides the integral of motion, one includes *arbitrary* functions of the BGT roots.

Introduction.— The issue of how statistical ensembles arise from the out-of-equilibrium dynamics in *isolated* quantum many-body system is still a fundamental, yet challenging, problem. The main motivation of the renewed interest in this topic is the high degree of control reached in out-of-equilibrium experiments with cold atomic gases[1–15]. The paradigm experiment is the so-called gloabal *quantum quench*[16], in which a system is initially prepared in an eigenstate $|\Psi_0\rangle$ of a many-body Hamiltonian $\mathcal{H}$. Then a global parameter of $\mathcal{H}$ is suddenly changed, and the system is let to evolve unitarily under the new Hamiltonian $\mathcal{H}'$. At long times after the quench the system equilibrates, as it is confirmed by experiments. On the other hand, in integrable models the presence of non-trivial *local* conserved quantities, besides the energy, strongly affects the dynamics and the nature of the steady state. As for now, despite the tremendous theoretical effort[23–60], it is still unclear wheather such steady-state can be described by a statistical ensemble, and how to construct it.

It has been proposed that the long-time stationary value of a generic local operator $\mathcal{O}$ is described by a Generalized Gibbs Ensemble[24,28] (GGE) as $\langle\mathcal{O}\rangle \equiv \mathrm{Tr}(\mathcal{O}\rho^{GGE})$. Here ρ^{GGE} extends the Gibbs density matrix by including all the local conserved quantities $\mathcal{I}_j$ (charges) as

$$\rho^{GGE} = Z^{-1} \exp\big(-\lambda_j \mathcal{I}_j\big). \qquad (1)$$

In (1), and in the rest of the paper, repeated indices are summed over. Z is a normalization factor. The λ_j are Lagrange multipliers to be fixed by imposing $\langle\Psi_0|\mathcal{I}_j|\Psi_0\rangle = \langle\mathcal{I}_j\rangle$, and $\mathcal{I}_2 = \mathcal{H}'$ is the post-quench Hamiltonian. In realistic situations one deals with the truncated GGE (TGGE), i.e., considering only a finite subset of the charges.

While the validity of the GGE has been largely confirmed in non-interacting field theories[41,43,50], in interacting ones the scenario is far less clear (see Ref. 53 for some results in an interacting spin chain). For Bethe ansatz solvable models the so-called quench-action method[56] allows for an exact treatement of the steady state, provided that the overlap between the initial state $|\Psi_0\rangle$ and the eigenstates of $\mathcal{H}'$ are known. Surprisingly, in several cases the quench-action is in disagreement with the TGGE[57–60], whereas it seems to be supported by numerical simulations[57]. While one might argue that the GGE can be "repaired" by enlarging the set of charges included in (1), no quantitative study in this direction has been conducted yet. One intriguing possibility is that local charges are not sufficient, and one has to include quasi-local ones[20–22].

On the other hand, numerical methods, such as the time dependent density matrix renormalization group[17,18] (tDMRG), have been mostly used to simulate the post-quench dynamics in microscopic models. However, no numerical attempt to explore the GGE *per se* has been undertaken yet. The aim of this work is to provide a Monte-Carlo-based framework for studying the GGE, and its possible extensions, in Bethe ansatz solvable models. Although we restrict ourselves to finite-size systems, thermodynamic quantities can be extracted by a standard finite-size scaling analysis. Moreover, as finite-size corrections decay exponentially with system size, moderately large systems are sufficient to access the thermodynamic limit. The method relies on the detailed knowledge of the Hilbert space structure provided by the Bethe ansatz formalism, and on the Bethe-Gaudin-Takahashi (BGT) equations[63,64]. The key idea is to sample the model Hilbert space according to the GGE probability measure given in (1). We should mention that the same idea has been already explored in Ref. 69 for the Gibbs ensemble. The method allows one to obtain GGE expectation value for generic observables, provided that their expression in terms of the roots of the BGT equations are known. Remarkably, it is also possible to extract the steady-state roots distributions, which encode the complete information about ensemble averages in the thermodynamic limit. It is also straightforward to extend the GGE including in (1) arbitrary functions of the BGT roots, besided the $\mathcal{I}_j$. This could be useful, for instance, to investigate the effects of quasi-local charges. Finally, we should mention that, in principle, GGE averages of local observables can be computed using exact diagonalization or Quantum Monte Carlo. However, both these methods require the operatorial expression of the conserved charges (see Re. 19 for the XXX chain), whereas our approach relies only on their expression (typically simple) in terms of the BGT roots.

We benchmark the approach focusing on the spin-$\frac{1}{2}$ isotropic Heisenberg chain (XXX chain), which is the ven-

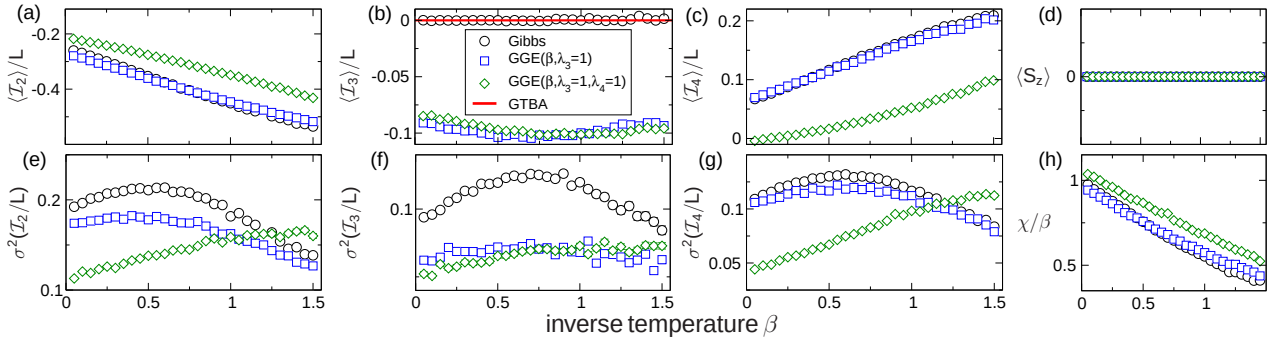

FIG. 1. The Generalized Gibbs Ensemble (GGE) for the Heisenberg spin chain with $L = 16$ sites: numerical results obtained using the Hilbert space Monte Carlo sampling approach. Only the first three conserved charges $\mathcal{I}_j$ ($j = 1, 2, 3$) are included in the GGE. $\mathcal{I}_2$ is the Hamiltonian. In all the panels different symbols correspond to different values of the Lagrange multipliers λ_3, λ_4. The circles correspond to the Gibbs ensemble, i.e., $\lambda_3 = \lambda_4 = 0$. The x-axis shows the inverse temperature $\lambda_2 = \beta$. (a) The GGE average $\langle \mathcal{I}_2/L \rangle$. (b) Variance of the GGE fluctuations $\sigma^2(\mathcal{I}_2/L) \equiv \langle (\mathcal{I}_2/L)^2 \rangle - \langle \mathcal{I}_2/L \rangle^2$ as a function of β. (c)(d) and (e)(f): Same as in (a)(b) for $\mathcal{I}_3$ and $\mathcal{I}_4$, respectively. In all panels the dash-dotted lines are the Generalized Thermodynamic Bethe Ansatz (GTBA) results. (g) The GGE expectation value of the total magnetization $\langle S_z \rangle$. Notice that $\langle S_z \rangle = 0$ due to the $SU(2)$ invariance of the conserved charges. (h) χ/β plotted versus β, with χ being the magnetic susceptibility per site.

erable prototype of integrable models[61]. We consider several TGGEs (cf. (1)) constructed including $\mathcal{I}_2, \mathcal{I}_3, \mathcal{I}_4$, and varying the associated Lagrange multipliers λ_j. We focus on the conserved charges averages $\langle \mathcal{I}_j/L \rangle$ and their ensemble fluctuations $\sigma^2(\mathcal{I}_j/L) \equiv \langle (\mathcal{I}_j/L)^2 \rangle - \langle \mathcal{I}_j/L \rangle^2$. All these quantities are related to well-known physical observables, such as the energy density, the energy current per site, the specific heat, and the thermal Drude weight[70]. We also compute the average magnetization and the spin susceptibility per site χ/L. Already for a chain with $L = 20$ sites the Monte Carlo data perfectly agree with the Generalized Thermodynamic Bethe Ansatz (GTBA) approach. We stress that this is the first direct numerical check of the GTBA for the XXX chain. Finally, we extract the BGT roots distributions for the Gibbs ensemble at several temperatures, and the GGE. For both ensembles the finite-size effects are negligible for small roots, which are the relevant ones to describe the long-wavelength physics. For the Gibbs ensemble we compare our numerical data with standard finite-temperature Thermodynamic Bethe Ansatz (TBA) results, finding excellent agreement.

The-Heisenberg-spin-chain.— The isotropic spin-$\frac{1}{2}$ Heisenberg (XXX) chain with L sites is defined by the Hamiltonian

$$\mathcal{H} \equiv J \sum_{i=1}^{L} \left[\frac{1}{2}(S_i^+ S_{i+1}^- + S_i^- S_{i+1}^+) + S_i^z S_{i+1}^z \right], \quad (2)$$

where $S_i^{\pm} \equiv (\sigma_i^x \pm i\sigma_i^y)/2$ are spin operators acting on the site i, $S_i^z \equiv \sigma_i^z/2$, and $\sigma_i^{x,y,z}$ the Pauli matrices. We fix $J = 1$ and use periodic boundary conditions, identifying sites $L + 1$ and 1. The total magnetization $S_T^z \equiv \sum_i S_i^z = L/2 - M$, with M number of down spins (particles), commutes with (2), and it is here used to label the XXX chain eigenstates.

In the Bethe ansatz formalism each eigenstate of (2) is univocally identified by M parameters $\{x_\alpha \in \mathbb{C}\}_{\alpha=1}^M$. In the limit $L \to \infty$ they form "string" patterns along the imaginary axis of the complex plane (string hypothesis)**cita Bethe Takahashi**. Strings of length $1 \le n \le M$ (so-called n-strings) are parametrized as $x_{n;\gamma}^j = x_{n;\gamma} - i(n - 1 - 2j)$. Here $x_{n;\gamma} \in \mathbb{R}$ is the string real part (string center), $j = 0, 1, \ldots, n-1$ labels different string components, and γ denotes different string centers. The string hypothesis is not correct for finite chains, although deviations typically decay exponentially with L. Physically, the n-strings correspond to eigenstate components containing n-particle bound states. The $\{x_{n;\gamma}\}$ are the roots of the Bethe-Gaudin-Takahashi (BGT) equations

$$L\vartheta_n(x_{n;\gamma}) = 2\pi I_{n;\gamma} + \sum_{(m,\beta)\neq(n,\gamma)} \Theta_{m,n}(x_{n;\gamma} - x_{m;\beta}). \quad (3)$$

Here $\vartheta_n(x) \equiv 2\arctan(x/n)$, $\Theta_{m,n}(x)$ is the scattering phase between different roots, and $I_{n;\gamma} \in \frac{1}{2}\mathbb{Z}$ are the so-called Bethe-Takahashi quantum numbers. The $I_{n;\gamma}$ satisfy the upper bound $|I_{n;\gamma}| \le I_{\rm MAX}(n, L, M)$, with $I_{\rm MAX}$ a known function of n, M, L[64]. Every choice of $I_{n;\gamma}$ identifies an eigenstate of (2). The "string content" of each eigenstate is denoted as $\mathcal{S} \equiv \{s_1, \ldots, s_M\}$, with $0 \le s_n \le \lfloor M/n \rfloor$ the number of n-strings. The conserved charges $\mathcal{I}_j$ of the XXX chain are given as

$$\mathcal{I}_{j+1} \equiv \frac{i}{(j-1)!} \frac{d^j}{dy^j} \log \Lambda(y) \Big|_{y=i}, \quad (4)$$

where $\Lambda(y)$ is the eigenvalue of the quantum transfer matrix[65], with y a spectral parameter. $\mathcal{I}_2$ is the XXX hamiltonian. The exact expression of the charges in terms of spin operators is known explicitly for $j \le 10$[19]. Larger values of j in (4) correspond to less local charges. Precisely, the support of $\mathcal{I}_j$, i.e., the number of adjacent sites where $\mathcal{I}_j$ acts non trivially, increases linearly with j. The eigenvalues of $\mathcal{I}_j$ on a generic eigenstate are obtained by summing the contributions of the different BGT roots *independently*. For instance, the energy is obtained as $E = 2\sum_{n,\gamma} n/(n^2 + x_{n;\gamma}^2)$. Similar results are obtained for other charges using (4).

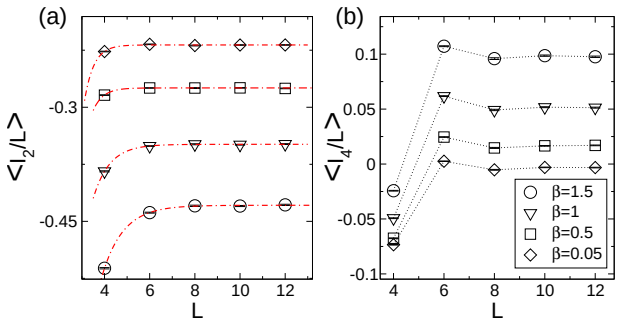

FIG. 2. Finite-size scaling of the GGE averages in the Heisenberg chain: Numerical results obtained from the Hilbert space Monte Carlo sampling. Here the GGE is constructed including $\mathcal{I}_2, \mathcal{I}_3, \mathcal{I}_4$, with Lagrange multipliers $\lambda_2 = \beta, \lambda_3 = \lambda_4 = 1$. (a) $\langle \mathcal{I}_2/L \rangle$ plotted versus the chain size L for several values of β. The dash-dotted lines are exponential fits. (b) Same as in (a) for $\mathcal{I}_4$.

The-Hilbert-space-Monte-Carlo-sampling.— For a finite chain the GGE ensemble (1) can be simulated by sampling the eigenstates of (2). One starts with an initial M-particle eigenstate, with string content $\mathcal{S} = \{s_1, \ldots, s_M\}$, and identified by a BGT quantum number configuration $\mathcal{C} = \{I_{n;\gamma}\}_{n=1}^{M}$ ($\gamma = 1, \ldots, s_n$). The corresponding charges eigenvalues are $\{\mathcal{I}_j\}$. Then a new eigenstate is generated with a Monte Carlo scheme. Each Monte Carlo step (mcs) consists of three moves:

1. Choose a new particle number sector M', and string content $\mathcal{S}'$ with probability $\mathcal{P}(M', \mathcal{S}')$.

2. Generate a new quantum number configuration $\mathcal{C}'$ compatible with the $\mathcal{S}'$ obtained in step 1. Solve the corresponding BGT equations (3).

3. Calculate the charge eigenvalues $\mathcal{I}'_j$ and accept the new eigenstate with the Metropolis probability:

$$\mathrm{Min}\Big\{1, \frac{L-2M'+1}{L-2M+1} e^{-\lambda_j(\mathcal{I}'_j - \mathcal{I}_j)}\Big\}. \tag{5}$$

In (5) the factor in front of the exponential takes into account that $\mathcal{I}_j$ are invariant under $SU(2)$ rotations. Crucially, the steps 1 and 2 are necessary to account correctly for the density of states of the model, and are the same for the Gibbs ensemble[69]. The iteration of 1-3 defines a Markov chain, which, after some thermalization steps, generates eigenstates sampled according to (1). Clearly, it is straightforward to simulate the GGE with fixed particle number M. More interestingly, by trivially modifying (5) it is possible to simulate more exotic ensembles in which, in addtion to $\mathcal{I}_j$, one considers arbitrary functions of the BGT roots. This could be useful to include the quasi-local charges in the GGE. The ensemble average $\langle \mathcal{O} \rangle$ of a generic operator is obtained as

$$\langle \mathcal{O} \rangle = \lim_{N_{\rm mcs}\to\infty} \frac{1}{N_{\rm mcs}} \sum_{|s\rangle} \langle s|\mathcal{O}|s\rangle, \tag{6}$$

where $N_{\rm mcs}$ is the total number of eigenstates $|s\rangle$ sampled in the Monte Carlo. Moreover, for all the observables considered here the contributions of the roots can be summed independently, i.e.,

$$\langle s|\mathcal{O}|s\rangle = \sum_{n,\gamma} f_{\mathcal{O}}(x_{n;\gamma}) \tag{7}$$

where $x_{n;\gamma}$ are the BGT roots identifying the eigenstate $|s\rangle$, and $f_{\mathcal{O}}(x)$ depends on the observable.

The-GGE-for-local-observables.— The correctness of the Monte Carlo approach is illustrated in Fig. 1, considering the charge densities $\langle \mathcal{I}_j/L \rangle$ (panels (a)-(c) in the Figure), and the variance of their ensemble fluctuations $\sigma^2(\mathcal{I}_j/L) \equiv \langle (\mathcal{I}_j/L)^2 \rangle - \langle \mathcal{I}_j/L \rangle^2$ (panels (e)-(g)). Panels (d)(h) plot the total magnetization $\langle S_z \rangle$, i.e., the average particle number, and χ/β, with χ the spin susceptibility. Notice that $\langle \mathcal{I}_2/L \rangle$ is the energy density, $\langle \mathcal{I}_3/L \rangle$ the energy current per site, while $\sigma^2(\mathcal{I}_2/L)$ and $\sigma^2(\mathcal{I}_3/L)$ are related to the specific heat, and the thermal Drude weight, respectively. In all panels the data correspond to the TGGE constructed with the first three charges $\mathcal{I}_2, \mathcal{I}_3, \mathcal{I}_4$. Different symbols correspond to different values of the associated Lagrange multipliers, namely $\lambda_3 = \lambda_4 = 0$ (Gibbs ensemble, circles in the Figure), $\lambda_3 = 1$ and $\lambda_4 = 0$ (squares), and $\lambda_3 = \lambda_4 = 1$ (rhombi). In all panels the x-axis shows the inverse temperature $\lambda_2 = \beta$. The data are Monte Carlo averages with $N_{\rm mcs} = 5 \cdot 10^5$ (cf. (6)). As expected, the different ensemble give different expectation values, implying that the local observables we consider are able to distinguish different GGEs. In panel (b) $\langle \mathcal{I}_3 \rangle = 0$ for the Gibbs ensemble due to parity symmetry, while in (d) $\langle S_z \rangle = 0$ due to the $SU(2)$ symmetry of (2). In Fig. 1 the continuous lines are the analyitic results obtained in the thermodynamic limit by solving the $GTBA$ equations. These fully match the Monte Carlo data, signaling that finite-size effects are negligible already for $L = 16$.

The finite-size corrections are more carefully investigated in Fig. 2, plotting $\langle \mathcal{I}_2 \rangle$ and $\langle \mathcal{I}_4 \rangle$ (panels (a) and (b), respectively) versus β. Here we focus on the $TGGE$ with $\lambda_2 = \beta, \lambda_3 = 0$ and $\lambda_4 = 1$. Clearly, finite-size effects decay exponentially with L for any β. In (a) the dashed lines are fits to $c_1 + c_2 \exp(-c_3 L)$, with c_1, c_2, c_3 fitting parameters. Moreover, corrections are larger at lower temperature, and increase with the range of the operator (compare panels (a) and (b) in Fig. 2).

Extracting-the-root-distributions.— In the thermodynamic limit in each n-string sector the roots of (3) become dense. Thus, instead of the eigenstates, one considers the corresponding root distributions $\boldsymbol{\rho} \equiv \{\rho_n\}_{n=1}^{\infty}$. Formally, one has $\rho_n \equiv \lim_{L\to\infty}[L(x_{n;\gamma+1} - x_{n;\gamma})]^{-1}$. For a generic observable $\mathcal{O}$, the GGE average becomes a functional integral as

$$\mathrm{Tr}\big\{ \exp\big(\lambda_j \mathcal{I}_j\big)\mathcal{O}\big\} \to \int \mathcal{D}\boldsymbol{\rho} \exp\big(S[\boldsymbol{\rho}] + \lambda_j \mathcal{I}_j[\boldsymbol{\rho}]\big)\mathcal{O}[\boldsymbol{\rho}]. \tag{8}$$

Here $S[\boldsymbol{\rho}]$ is the Yang-Yang entropy, which counts the number of eigenstates leading to the same $\boldsymbol{\rho}$, and it is extensive. In (8) it is assumed that $\mathcal{O}$ becomes a smooth functional of $\boldsymbol{\rho}$ in the thermodynamic limit. In particular, (7) becomes

$$\langle s|\mathcal{O}|s\rangle \to \sum_n \int dx \rho_n(x) f_{\mathcal{O}}(x). \tag{9}$$

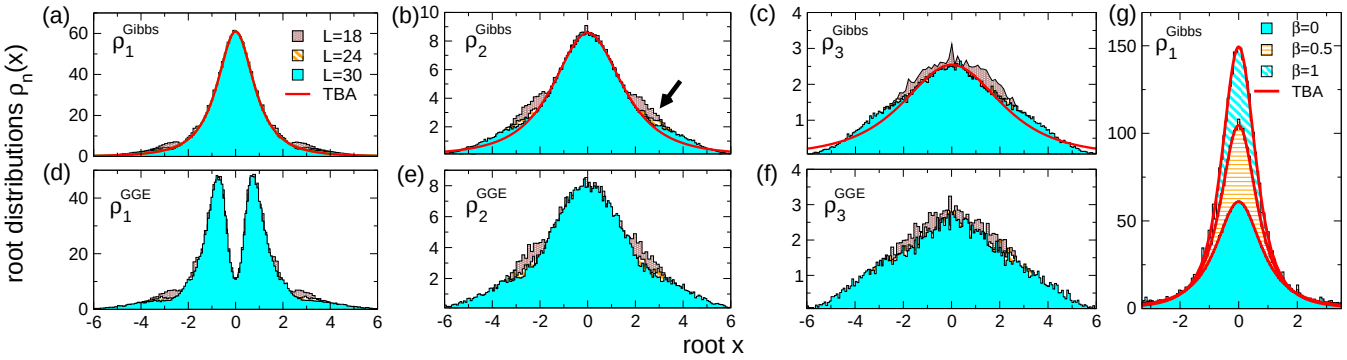

FIG. 3. The root distributions $\rho_n(x)$ (for $n = 1, 2, 3$) for the infinite temperature Gibbs (panels (a)-(c)) and the GGE equilibrium states (panels (d)-(f)): Numerical results for the Heisenberg spin chain obtained using the Hilbert space Monte Carlo sampling. Here the GGE is constructed including only $\mathcal{I}_2$ and $\mathcal{I}_4$ with fixed Lagrange multipliers $\lambda_2 = 0$ and $\lambda_4 = 1$. In all the panels the data are the histograms of the n-strings roots sampled in the Monte Carlo. The width of the histogram bins is $\Delta x = 2/L$, with L the chain size. In each panel different histograms correspond to different L. All the data are divided by 10^3 for convenience. In (b) the arrow highlights the finite-size effects. In (a)-(c) the lines are the Thermodynamic Bethe Ansatz (TBA) results. (g) Finite-temperature effects: Monte Carlo data for ρ_1^{Gibbs} for different values of the inverse temperature β.

Since both $S[\boldsymbol{\rho}]$ and $\mathcal{I}_j[\boldsymbol{\rho}]$ are extensive, the functional integral in (8) is dominated by the saddle point $\boldsymbol{\rho}^{sp}$, with $\delta(S + \lambda_j \mathcal{I}_j)/\delta\boldsymbol{\rho}|_{\boldsymbol{\rho}=\boldsymbol{\rho}^{sp}} = 0$. Here $\boldsymbol{\rho}^{sp}$ acts as a representative state for the ensemble, and it contains the full information about the GGE equilibrium steady state. Eq. (6) and (9) imply that in the thermodynamic limit the histograms of the BGT roots sampled in the Monte Carlo converge to ρ_n^{sp}.

This is supported in Fig. 3 considering several GGEs. Panels (a)-(c) plot the root distributions $\rho_n^{sp}(x)$ for $n = 1, 2, 3$ as a function of x for the representative state (saddle point) of the infinite-temperature Gibbs ensemble. In each panel the different histograms correspond to different chain sizes $18 \leq L \leq 30$. The data are obtained using $5 \cdot 10^5$ Monte Carlo steps. The width of the histogram bins is varied with L as $2/L$. In all the panels the full lines are the analytical Thermodynamic Bethe Ansatz[64] (TBA) results. Clearly, deviations from the TBA vanish upon increasing the chain size (see for instance the arrow in panel (b)). Moreover, the corrections are larger on the tails of the distributions. This is expected since large roots correspond to large quasi-momenta, which are more sensitive to the lattice effects. Finally, finite-size effects increase with n, i.e., with the bound state sizes, as expected. The results for the finite-temperature Gibbs ensemble are presented in Fig. 1 (g), for $\beta = 1/2$ and $\beta = 1$ (the different histograms). We focus on $\rho_1(x)$, restricting ourselves to $L = 30$. The infinite temperature histogram is reported for comparison. The continuous lines are now finite-temperature TBA results, and perfectly agree with the Monte Carlo data. Upon lowering the temperature the height of the peak at $x = 0$ increases. This reflects that at $\beta = \infty$ the tail of the root distributions vanish exponentially, whereas for $\beta = 0$ they are $\sim 1/x^4$[64]. Finally, panels (d)-(f) plot $\rho_n(x)$ for the TGGE constructed with $\mathcal{I}_2, \mathcal{I}_4$ at fixed $\lambda_2 = 0$, $\lambda_4 = 1$ and for $L = 30$. Interestingly, in contrast with the thermal case (see (a)), ρ_1 exhibits a double peak structure at small x. Similar to the infite-temperature Gibbs ensemble ((a)-(c) in the Figure), the data suggest that for $L = 30$ finite-size effects are negligible, at least for $-2 \leq x \leq 2$.

Conclusions.— We presented a Monte-Carlo-based scheme for simulating the truncated Generalized Gibbs ensemble (TGGE) in finite-size integrable models. The key idea is to sample the eigenstates of the model using the GGE probability measure. The method relies on the Bethe ansatz formalism, and, in particular, on the Bethe-Gaudin-Takahashi (BGT) equations. The thermodynamic limit can be accessed by standard finite-size scaling analysis. Remarkably, it is possible to extract in a simple way the steady-steate BGT root distributions, which contain full information about the (GGE) ensemble averages in the thermodynamic limit. Finally, it is possible to simulate extensions of the GGE, in which, besides the integral of motion, one includes arbitrary functions of the BGT roots. We bechmarked the method focusing on the spin-$\frac{1}{2}$ isotropic Heisenberg chain. We compared the numerical results with the Generalized Thermodynamic Bethe ansatz, finding excellent agreement. Moreover, for local quantities the finite-size corrections to the GGE expectation values decay exponentially with the chain size.

As an interesting research direction, we mention that it would be useful to simulate the GGE at fixed value of the conserved charges. This would be the same in spirit as what is done in microcanonical Monte Carlo simulations in lattice gauge theory[67] or molecular dynamics simulations[68]. It should be possible to employ the same techniques for the GGE.

Acknowledgements.— I would like to thank Maurizio Fagotti for providing the analytical GTBA results in Fig. 1 and Lorenzo Piroli for the finite-temperature TBA in Fig. 2. I would like to thank P. Calabrese, M. Fagotti, F. Essler, and L. Piroli, for useful discussions and comments. I acknowledge financial support by the ERC under Starting Grant 279391 EDEQS.

[1] I. Bloch, J. Dalibard, and W. Zwerger, Rev. Mod. Phys. **80**, 885 (2008).
[2] M. Greiner, O. Mandel, T. Hänsch, and I. Bloch, Nature (London) **419**, 51 (2002).
[3] T. Kinoshita, T. Wenger, and D. S. Weiss, Nature (London) **440**, 900 (2008).
[4] S. Hofferberth, I. Lesanovsky, B. Fischer, T. Schumm, and J. Schiedmayer, Nature (London) **449**, 324 (2007).
[5] S. Trotzky, Y.-A. Chen, A. Flesch, I. P. McCulloch, U. Schollwöck, J. Eisert, and I. Bloch, Nature Phys. **8**, 325 (2012).
[6] M. Gring, M. Kuhnert, T. Langen, T. Kitagawa, B. Rauer, M. Schreitl, I. Mazets, D. A. Smith, E. Demler, and J. Schmiedmayer, Science **337**, 6100 (2012).
[7] M. Cheneau, P. Barmettler, D. Poletti, M. Endres, P. Schaua, T. Fukuhara, C. Gross, I. Bloch, C. Kollath, and S. Kuhr, Nature (London) **481**, 484 (2012).
[8] U. Schneider, L. Hackeruller, J. P. Ronzheimer, S. Will, S. Braun, T. Best, I. Bloch, E. Demler, S. Mandt, D. Rasch, and A. Rosch, Nature Phys. **8**, 213 (2012).
[9] M. Kuhnert, R. Geiger, T. Langen, M. Gring, B. Rauer, T. Kitagawa, E. Demler, D. Adu Smith, and J. Schmiedmayer, Phys. Rev. Lett. **110**, 090405 (2013).
[10] T. Langen, R. Geiger, M. Kuhnert, B. Rauer, and J. Schmiedmayer, Nature Phys. **9**, 640 (2013).
[11] F. Meinert, M. J. Mark, E. Kirilov, K. Lauber, P. Weinmann, A. J. Daley, and H.-C. Nagerl, Phys. Rev. Lett. **111**, 053003 (2013).
[12] T. Fukuhara, A. Kantian, M. Endres, M. Cheneau, P. Schaua, S. Hild, C. Gross, U. Schollwöck, T. Giamarchi, I. Bloch, and S. Kuhr, Nature Phys. **9**, 235 (2013).
[13] J. P. Ronzheimer, M. Schreiber, S. Braun, S. S. Hodgman, S. Langer, I. P. McCulloch, F. Heidrich-Meisner, I. Bloch, and U. Schneider, Phys. Rev. Lett. **110**, 205301 (2013).
[14] S. Braun, M. Friesdorf, S. Hodgman, M. Schreiber, J. Ronzheimer, A. Riera, M. del Rey, I. Bloch, J. Eisert, and U. Schneider, PNAS **112**, 3641 (2015).
[15] T. Langen, S. Erne, R. Geiger, B. Rauer, T. Schweigier, M. Kuhnert, W. Rohringer, I. E. Mazets, T. Gasenzer, J. Schmiedmayer, Science **348**, 6231 (2015).
[16] A. Polkovnikov, K. Sengupta, A Silva, and M. Vengalattore, Rev. Mod. Phys. **83**, 863 (2011).
[17] S. R. White and A. E. Feiguin, Phys. Rev. Lett. **93**, 076401 (2004).
[18] A. J. Daley, C. Kollath, U. Schollock, and G. Vidal, J. Stat. Mech. (2004) P04005.
[19] M. P. Grabowski and P. Mathieu, Ann. Phys. N.Y. **243**, 299 (1995).
[20] T. Prosen, Nucl. Phys. B **886**, (2014) 1177.
[21] R. G. Pereira, V. Pasquier, J. Sirker, and I. Affleck, J. Stat. Mech. (2014) P09037.
[22] E. Ilievski, M. Medejak, and T. Prosen, arXiv:1506.05049.
[23] P. Calabrese and J. Cardy, Phys. Rev. Lett. **96**, 136801 (2006).
[24] M. Rigol, V. Dunjko, V. Yurovsky, and M. Olshanii, Phys. Rev. Lett. **98**, 050405 (2007).
[25] P. Calabrese and J. Cardy, J. Stat. Mech. (2007) P06008.
[26] C. Kollath, A. M. Läuchli, and E. Altman, Phys. Rev. Lett. **98**, 180601 (2007).
[27] S. R. Manmana, S. Wessel, R. M. Noack, and A. Muramatsu, Phys. Rev. Lett. **98**, 210405 (2007).
[28] M. Rigol, V. Dunjko, and M. Olshanii, Nature **452**, 854 (2008).
[29] M. Cramer, C. M. Dawson, J. Eisert, and T. J. Osborne, Phys. Rev. Lett. **100**, 030602 (2008).
[30] T. Barthel and U. Schollwöck, Phys. Rev. Lett. **100**, 100601 (2008).
[31] M. Kollar and M. Eckstein, Phys. Rev. A **78**, 013626 (2008).
[32] M. Moeckel and S. Kehrein, Phys. Rev. Lett. **100**, 175702 (2008).
[33] A. Iucci and M. A. Cazalilla, Phys. Rev. A **80**, 063619 (2009).
[34] D. Rossini, A. Silva, G. Mussardo, and G. E. Santoro, Phys. Rev. Lett. **102**, 127204 (2009).
[35] P. Barmettler, M. Punk, V. Gritsev, E. Demler, and E. Altman, Phys. Rev. Lett. **102**, 130603 (2009).
[36] G. Biroli, C. Kollath, and A. M. Läuchli, Phys. Rev. Lett. **105**, 250401 (2010).
[37] D. Rossini, S. Suzuki, G. Mussardo, G. E. Santoro, and A. Silva, Phys. Rev. B **82**, 144302 (2010).
[38] D. Fioretto and G. Mussardo, New J. Phys. **12**, 055015 (2010).
[39] C. Gogolin, M. P. Mueller, and J. Eisert, Phys. Rev. Lett. **106**, 040401 (2011).
[40] M. C. Bañuls, J. I. Cirac, and M. B. Hastings, Phys. Rev. Lett. **106**, 050405 (2011).
[41] P. Calabrese, F. H. L. Essler, and M. Fagotti, Phys. Rev. Lett. **106**, 227203 (2011).
[42] M. Rigol and M. Fitzpatrick, Phys. Rev. A **84**, 033640 (2011).
[43] P. Calabrese, F. H. L. Essler, and M. Fagotti, J. Stat. Mech. (2012) P07016.
[44] J.-S. Caux and R. M. Konik, Phys. Rev. Lett. **109**, 175301 (2012).
[45] F. H. L. Essler, S. Evangelisti, and M. Fagotti, Phys. Rev. Lett. **109**, 247206 (2012).
[46] M. A. Cazalilla, A. Iucci, and M.-C. Chung, Phys. Rev. E **85**, 011133 (2012).
[47] J. Mossel and J.-S. Caux, New J. Phys. **14** 075006 (2012).
[48] M. Collura, S. Sotiriadis and P. Calabrese, Phys. Rev. Lett. **110**, 245301 (2013)
[49] G. Mussardo, Phys. Rev. Lett. **111**, 100401 (2013).
[50] M. Fagotti and F. H. L. Essler, Phys. Rev. B **87**, 245107 (2013).
[51] S. Sotiriadis and P. Calabrese, J. Stat. Mech. (2014) P07024.
[52] F. H. L. Essler, S. Kehrein, S. R. Manmana, and N. J. Robinson, Phys. Rev. B **89**, 165104 (2014).
[53] M. Fagotti, M. Collura, F. H. L. Essler, and P. Calabrese, Phys. Rev. B **89**, 125101 (2014).
[54] T. M. Wright, M. Rigol, M. J. Davis, and K. V. Kheruntsyan, Phys. Rev. Lett. **113**, 050601 (2014).
[55] G. Goldstein and N. Andrei, arXiv:1405.4224.
[56] J.-S. Caux and F. H. L. Essler, Phys. Rev. Lett. **110**, 257203 (2013).
[57] B. Pozsgay, M. Mestyán, M. A. Werner, M. Kormos, G. Zaránd, and G. Takács, Phys. Rev. Lett. **113**, 117203 (2014).
[58] B. Wouters, M. Brockmann, J. De Nardis, D. Fioretto, M. Rigol, and J.-S. Caux, Phys. Rev. Lett. **113**, 117202 (2014).
[59] J. De Nardis, B. Wouters, M. Brockmann, and J.-S. Caux, Phys. Rev. A **89**, 033601 (2014).
[60] M Mestyán, B. Pozsgay, G. Takács, and M. A. Werner, J. Stat. Mech. (2015) P04001.
[61] H. Bethe, Z. Phys. **71**, 205 (1931).
[62] C. N. Yang and C. P. Yang, J. Math. Phys. **10**, 1115 (1969).
[63] M. Takahashi, Prog. Theor. Phys. **46**, 401 (1971).
[64] M. Takahashi, *Thermodynamics of one-dimensional solvable models*, Cambridge University Press 1999.
[65] V. E. Korepin, N. M. Bogoliubov, and A. G. Izergin, *Quantum Inverse Scattering Methods and Correlation Functions*, Cambridge University Press 1997.
[66] J. Mossel and J.-S. Caux, J. Phys. A: Math. Theor. **45**, 255001 (2012).

[67] M. Creutz, Phys. Rev. Lett. **50**, 1411 (1983).
[68] R. Lustig, J. Chem. Phys. **109**, 8816 (1998).
[69] S.-J. Gu, N. M. R. Peres, Y.-Q. Li, Eur. Phys. J. B **48**, 157 (2005).
[70] A. Klümper anbd K. Sakai, J. Phys. A **35**, 2173 (2002).